Immunity
Article

Regulatory T Cell-Derived Interleukin-10 Limits Inflammation at Environmental Interfaces

Yuri P. Rubtsov,[1] Jeffrey P. Rasmussen,[1] Emil Y. Chi,[2] Jason Fontenot,[1] Luca Castelli,[1] Xin Ye,[5] Piper Treuting,[4] Lisa Siewe,[6] Axel Roers,[6] William R. Henderson Jr.,[5] Werner Muller,[7] and Alexander Y. Rudensky[1,3,*]
[1]Department of Immunology
[2]Department of Pathology
[3]Howard Hughes Medical Institute
[4]Department of Comparative Medicine
University of Washington School of Medicine, Seattle, WA 98195
[5]Center for Allergy and Immunology, Department of Medicine
University of Washington School of Medicine, Seattle, WA 98109
[6]Department of Dermatology, University of Cologne, Kerpener Str. 62, 50937 Cologne, Germany
[7]Faculty of Life Sciences, University of Manchester, Manchester M13 9PL, UK
*Correspondence: aruden@u.washington.edu
DOI 10.1016/j.immuni.2008.02.017

SUMMARY

The regulatory T (Treg) cells restrain immune responses through suppressor-function elaboration that is dependent upon expression of the transcription factor Foxp3. Despite a critical role for Treg cells in maintaining lympho-myeloid homeostasis, it remains unclear whether a single mechanism or multiple mechanisms of Treg cell-mediated suppression are operating in vivo and how redundant such mechanisms might be. Here we addressed these questions by examining the role of the immunomodulatory cytokine IL-10 in Treg cell-mediated suppression. Analyses of mice in which the Treg cell-specific ablation of a conditional IL-10 allele was induced by Cre recombinase knocked into the *Foxp3* gene locus showed that although IL-10 production by Treg cells was not required for the control of systemic autoimmunity, it was essential for keeping immune responses in check at environmental interfaces such as the colon and lungs. Our study suggests that Treg cells utilize multiple means to limit immune responses. Furthermore, these mechanisms are likely to be nonredundant, in that a distinct suppressor mechanism most likely plays a prominent and identifiable role at a particular tissue and inflammatory setting.

INTRODUCTION

A subset of $CD4^+$ T cells known as regulatory T cells is responsible for limiting tissue damage and inflammation associated with both innate and adoptive immune responses (Miyara and Sakaguchi, 2007; Shevach et al., 2001). Treg cells represent a dedicated cell lineage generated in the thymus; their development is dependent upon the expression of the transcription factor Foxp3 (Fontenot et al., 2003; Hori et al., 2003; Khattri et al., 2003). In mice, Foxp3 is restricted in its expression to Treg cells, and it therefore represents the best marker to date for this cell subset (Fontenot et al., 2005). Furthermore, genetic deficiency in Foxp3 leads to a highly aggressive fatal lymphoproliferative autoimmune disorder affecting multiple organs, and drug-induced ablation of Treg cells in neonatal or adult mice results in a similar disease (Fontenot and Rudensky, 2005; Kim et al., 2007). In humans, Foxp3 mutations result in development of an analogous fatal disorder dubbed IPEX (*I*mmune disregulation, *P*olyendocrinopathy, *E*nteropathy, *X*-linked). Autoimmune lesions associated with the Foxp3 deficiency are characterized by lymphadenopathy, splenomegaly, and severe pathology of the skin and gastrointestinal tract, as well as fulminant immune-mediated inflammation of multiple organs, including the liver, pancreas, muscles, and lungs (Brunkow et al., 2001; Wildin and Freitas, 2005). Recent studies indicate that Foxp3 expression is necessary for suppressor function: Genetically marked cells transcribing the *Foxp3* locus and lacking expression of the Foxp3 protein are unable to suppress immune responses in vivo and in vitro (Gavin et al., 2007; Lin et al., 2007). Furthermore, ablation of Foxp3 gene expression in mature peripheral Treg cells results in a loss of suppressor function (Williams and Rudensky, 2007).

Despite its major significance, Treg cell-mediated suppression is poorly understood from a mechanistic point of view. Over the last several years, numerous molecular and cellular mechanisms of suppression have been proposed in studies utilizing an antibody-mediated blockade of putative effector molecules or adoptive transfers of Treg cells isolated from mice genetically deficient in these molecules. However, the emerging picture remains confusing because none of the mechanisms have been unequivocally proven to operate in un-manipulated animals. Furthermore, it is not clear whether a single unique mechanism can account for various manifestations of Treg cell suppression or whether multiple mechanisms are needed for suppression to commence. It is also unknown whether distinct suppression mechanisms, either singly or cooperatively, control a particular type of inflammation in a specific location. For example, in vitro studies unequivocally demonstrated a requirement for cell-cell-contact-dependent Treg cell-mediated suppression and excluded a role for IL-10 and TGF-β, two major cytokines

with pronounced immunomodulatory and immunosuppressive function (Kullberg et al., 2005; Shevach et al., 2001; von Boehmer, 2005). In contrast, some in vivo studies suggested a role for TGF-β1 and IL-10 as effector molecules of Treg cell-mediated suppression of colitis (Asseman et al., 1999; Fahlen et al., 2005; Li et al., 2007; Powrie et al., 1996). However, both cytokines were found to be nonessential for in vivo suppression of autoimmune gastritis (Shevach et al., 2001). The studies implicating IL-10 in Treg-mediated suppression relied on adoptive transfer of $CD25^+CD4^+$ Treg cells isolated from IL-10-deficient donor mice and cotransferred with naive or immune $CD4^+$ T cells into lymphopenic hosts. A caveat for this experimental approach is that the inflammation induced by transferred T cells is greatly facilitated by their proliferation under lymphopenic conditions. In addition, lymphopenic conditions might not favor IL-10 production by "effector" nonregulatory T cells. The latter cells were shown to serve as a major source of IL-10 in some parasitic infections in mice and humans (Anderson et al., 2007; Jankovic et al., 2007; Nylen et al., 2007). Furthermore, contaminating IL-10-producing Foxp3-negative T cells are present at a low frequency in the splenic and lymph node $CD25^-CD4^+$ T cell populations used in a numerous transfer experiments (Kamanaka et al., 2006; Maynard et al., 2007). In addition, Foxp3-negative T cell populations, including the IL-10-expressing cell subset, are likely to have inferior proliferative potential compared to that of regulatory $Foxp3^+$ T cells capable of a very robust expansion in lymphopenic hosts (Gavin et al., 2002; Komatsu and Hori, 2007). Together, these considerations make it possible to hypothesize that, in unmanipulated animals, Foxp3-negative T cells might represent a key source of IL-10. Finally, in mice with a targeted insertion of the GFP coding sequence into the *Foxp3* gene locus and a concomitant disruption of Foxp3 protein expression, we found that GFP^+ T cells expressing this $Foxp3^{null}$ allele express high amounts of IL-10 mRNA and protein, yet lacked suppressor function (Gavin et al., 2007). Thus, the role for IL-10 as a suppressor molecule elaborated by $Foxp3^+$ Treg cells to control immune inflammation remains uncertain.

To directly investigate a role for IL-10 in Treg cell-mediated suppression, we generated $Foxp3^{YFP\text{-}Cre}$ mice, capable of Treg cell-specific inactivation of genes of interest, and crossed them with $Il10^{flox/flox}$ mice harboring a conditional *Il10* allele. We found that the selective disruption of IL-10 expression in Treg cells led to spontaneous colitis. Furthermore, $Il10^{flox/flox} \times Foxp3^{YFP\text{-}Cre}$ mice developed substantially augmented immune-response-associated inflammation and pathology in the skin and lungs. Thus, in unmanipulated animals, IL-10 produced by Treg cells plays an important role in suppressing immune inflammation at environmental interfaces. These results strongly suggest that Treg cells utilize multiple suppression mechanisms to control various aspects of inflammation, which is mediated by distinct immune cell types in different settings, and that a deficiency in any single mechanism of suppression is unlikely to be equivalent to a complete lack of regulatory T cells. Furthermore, our data suggest that specific mechanisms of suppression do not operate in a completely redundant fashion and that these mechanisms, upon elucidation of their distinct contribution to Treg cell-mediated suppression, can be harnessed for potential therapeutic interventions.

RESULTS

Generation and Characterization of $Foxp3^{YFP\text{-}Cre}$ Mice

To generate mice capable of selective gene inactivation in Treg cells, we utilized gene targeting to insert the DNA sequence coding for a viral IRES followed by YFP-Cre recombinase fusion protein into the 3′ UTR of the *Foxp3* locus (Figure 1A). Chimeric males harboring the targeted $Foxp3^{YFP\text{-}Cre}$ allele were bred with female mice expressing the FLPe recombinase transgene to excise the Neo^r cassette and to confirm germ-line transmission of the targeted allele (Figure 1B). The Neo^r-negative progeny was crossed to C57BL/6 mice, and the resulting $Foxp3^{YFP\text{-}Cre}$ mice were analyzed for expression of the YFP-Cre and Foxp3 protein (Figure 1C). The YFP-Cre fusion protein expression was limited to Treg cells. To examine the specificity of Cre-mediated recombination in $Foxp3^{YFP\text{-}Cre}$ mice, we introduced the ROSA26YFP (R26Y) recombination reporter allele into these mice. This allele allowed for the detection of Cre-mediated recombination at a single-cell level through flow-cytometric analyses of YFP expression induced upon Cre-mediated excision of a "floxed" transcriptional stop cassette preceding the YFP coding sequence inserted into the ubiquitously expressed ROSA26 locus. Because the YFP reporter expression was markedly higher than that of the YFP-Cre fusion protein, essentially 100% efficient Cre-mediated recombination in $Foxp3^{YFP\text{-}Cre}$ Treg cells was readily ascertained upon costaining for CD4, CD8, and Foxp3. In addition, individual $Foxp3^{YFP\text{-}Cre}$ mice exhibited varying degrees (2%–10%) of R26Y recombination in different hematopoietic lineage cells that lacked detectable YFP-Cre and Foxp3 expression; such cells included immature and mature B cells, T cells, myeloid cells, and bone marrow precursor cells (Figure S1; data not shown). This was probably due to stochastic recombination events resulting from a basal level of $Foxp3^{YFP\text{-}Cre}$ transcription, consistent with the emerging data on the pervasive transcription of genes, including "silent" genes and non-coding sequences in addition to actively transcribed genes, involved in developmental processes within the genome (Guenther et al., 2007). However, the "off-target" recombination in $Foxp3^{YFP\text{-}Cre}$ mice was probably negligible in light of the fact that a recombination event affecting a single R26Y allele resulted in YFP expression, whereas ablation of a "floxed" gene of interest in homozygous configuration required deletion of both alleles.

Il10 Ablation in Treg Cells Does Not Perturb Their Development or Result in Systemic Autoimmunity

To generate mice in which the IL-10 deficiency was limited to Treg cells, we bred $Il10^{flox/flox}$ mice harboring loxP sites flanking the first exon of the *Il10* gene with $Foxp3^{YFP\text{-}Cre}$ mice. Genomic PCR-based examination of the wild-type ($Il10^{WT}$) as well as "floxed" intact ($Il10^{flox}$) and recombined ($Il10^{\Delta}$) alleles of the *Il10* gene in FACS-purified YFP^+CD4^+ and YFP^-CD4^+ T cells showed a highly efficient deletion in YFP^+CD4^+ T cells, i.e., $Foxp3^+$ Treg cells, in male $Il10^{flox/flox} \times Foxp3^{YFP\text{-}Cre}$ hemizygous mice, whereas the $Il10^{\Delta}$ allele was undetectable in YFP^- "non-Treg" $CD4^+$ T cells (see sorting gate in Figure S2). In addition, similar analysis of heterozygote $Il10^{flox/WT}$ $Foxp3^{YFP\text{-}Cre}$ mice reveals both the intact $Il10^{flox}$ and $Il10^{WT}$ alleles in $YFP\text{-}Cre^-$ non-Treg cells, whereas $YFP\text{-}Cre^+$ Treg cells contained

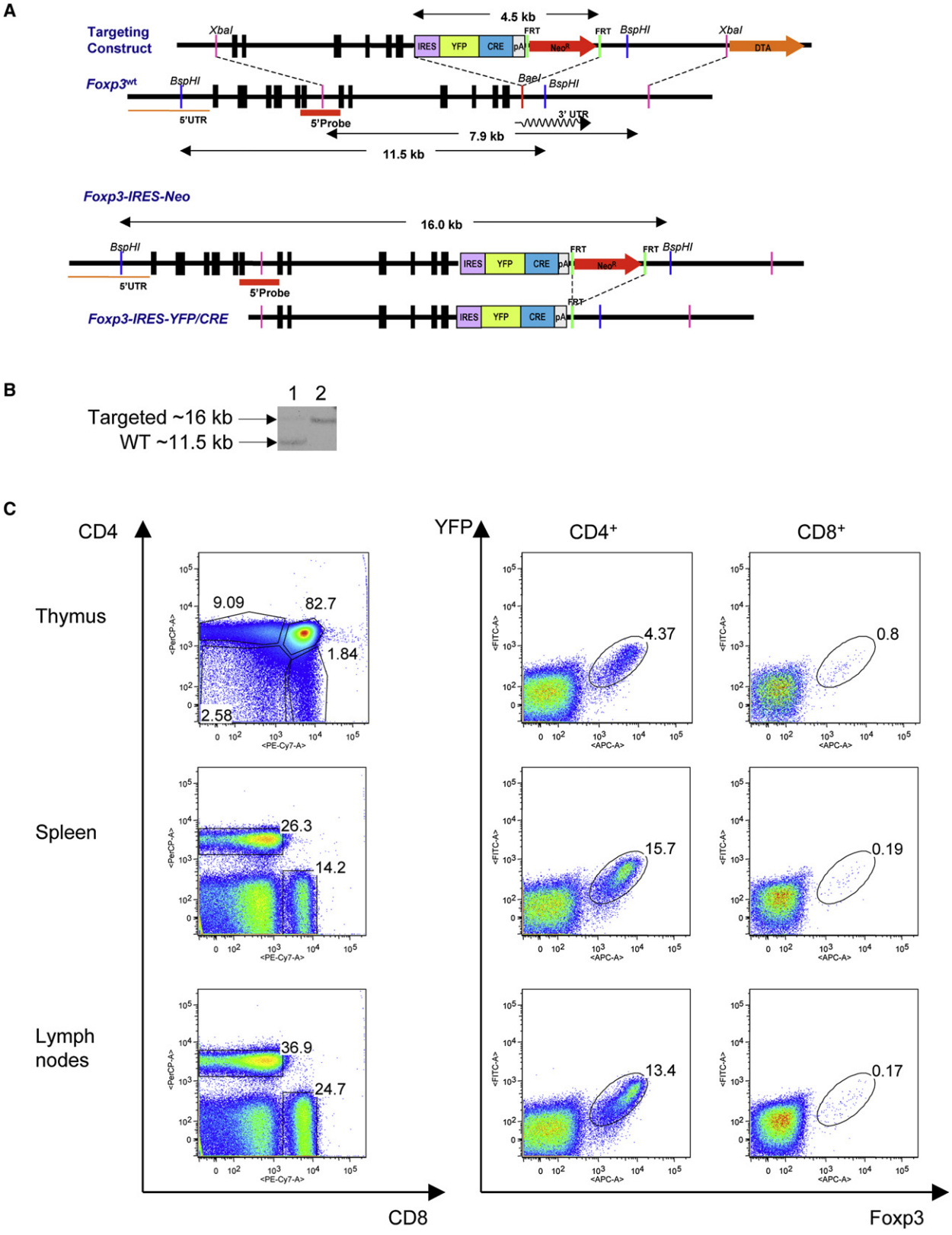

Figure 1. Generation and Characterization of Knock-In Mice Harboring the *Foxp3*$^{YFP\text{-}Cre}$ Allele
(A) The targeting strategy and map of the *Foxp3*$^{YFP\text{-}Cre}$ construct.

Il10^{WT} and *Il10*$^{\Delta}$ (Figure 2A). We estimated the degree of *Il10*^{flox} allele deletion to be at least 90% in YFP^{+} cells and undetectable in YFP^{-} cells (Figure 2B). To test the specificity of *Il10*^{flox} allele deletion at the protein level, we stimulated splenocytes from *Il10*$^{flox/flox}$ × *Foxp3*$^{YFP\text{-}Cre}$ and littermate control *Il10*$^{flox/WT}$ × *Foxp3*$^{YFP\text{-}Cre}$ mice in vitro and stained them intracellularly with Foxp3 and IL-10 antibodies (Figure S3A). We observed that IL-10-producing cells were greatly diminished within the Foxp3-expressing, but not Foxp3-negative, CD4^{+} T cell subset.

Male *Il10*$^{fl/fl}$ × *Foxp3*$^{YFP\text{-}Cre}$ and female *Il10*$^{fl/fl}$ × *Foxp3*$^{YFP\text{-}Cre/YFP\text{-}Cre}$ mice were born at a Mendelian frequency and lacked splenomegaly, lymphadenopathy or other detectable signs of autoimmune pathology up to 8 weeks of age (Figure 2C). Flow-cytometric analysis of mutant mice revealed numerically unaltered thymic and peripheral CD8^{+} and CD4^{+} T cell subsets, including Foxp3^{+} T cell subsets (Figure 2D). Further examination of the expression of several T cell activation markers on the surface of CD4^{+} T cells isolated from the lymph nodes, spleens, and mesenteric lymph nodes of mutant and control mice did not reveal noticeable differences (Figure 2E). IL-2, IL-4, IFN-γ, and TNF-α production by CD4^{+} T cells was also unaffected in 6- to 8-week-old *Il10*$^{flox/flox}$ × *Foxp3*$^{YFP\text{-}Cre}$ mice (Figure 2F). These observations were consistent with the largely intact suppressor capacity of Treg cells in these mice; a complete Treg cell deficiency due to loss-of-function or null *Foxp3* mutations or due to drug-induced ablation of the Treg cell subset results in a massive boost of cytokine production by T cells and lymphoproliferation. In agreement with these results, we failed to observe major signs of tissue pathology upon histologic examination of various organs of un-manipulated *Il10*$^{flox/flox}$ × *Foxp3*$^{YFP\text{-}Cre}$ mice, except for colon inflammation in older animals (see below). These results suggest that IL-10 expression by Treg cells is not essential for their requisite role in restraining early-onset systemic autoimmunity.

Il10$^{flox/flox}$ × Foxp3$^{YFP\text{-}Cre}$ Mice Develop Spontaneous Colitis

It has been shown that mice with the germ-line (*Il10*$^{-/-}$) or T cell-specific ablation of the *Il10* gene (*Il10*$^{flox/flox}$ × CD4-Cre) develop spontaneous inflammation in the intestine, in which *Helicobacter sp.* plays a prominent role. In one study, up to 40% of *Il10*$^{-/-}$ mice and a slightly smaller percentage of *Il10*$^{fl/fl}$ × CD4-Cre mice 6 months of age or older developed rectal prolapse indicative of severe colitis that showed some similarity to inflammatory bowel disease in human patients (Roers et al., 2004). To examine whether Treg cell-specific deficiency in IL-10 results in spontaneous colitis, we monitored a cohort of *Il10*$^{flox/flox}$ × *Foxp3*$^{YFP\text{-}Cre}$ and littermate control *Il10*$^{flox/WT}$ × *Foxp3*$^{YFP\text{-}Cre}$ mice for clinical signs of colitis, including rectal prolapse and diarrhea. As a positive control in these experiments, we used a cohort of *Il10*$^{-/-}$ mice. We found that starting at 10 weeks of age, *Il10*$^{flox/flox}$ × *Foxp3*$^{YFP\text{-}Cre}$ animals, but not the control group, presented with gross manifestations of colitis. Upon further examination of the affected animals, we found diffuse colonic thickening and a substantial increase in the size of the mesenteric lymph nodes and the spleen (data not shown). Blinded histological evaluation of sections of the stomach and the small and large intestine from the *Il10*$^{flox/flox}$ × *Foxp3*$^{YFP\text{-}Cre}$ mice showed that although the stomach and small intestine were not affected by IL-10 deficiency in Treg cells when these mice were compared to control mice, the large intestine, especially the cecum, showed prominent mononuclear infiltration of epithelial tissue as well as tissue destruction (Figures 3A and 3B). Colonic inflammation observed in *Il10*$^{flox/flox}$ × *Foxp3*$^{YFP\text{-}Cre}$ mice was histologically similar to that observed in *Il10*$^{-/-}$ mice, albeit that in the latter experimental group, the inflammation was more profuse and affected the entire length of the colon (Figures 3A and 3B). In agreement with microscopic observations, the onset of the disease was slightly delayed and the incidence was somewhat lower in *Il10*$^{flox/flox}$ × *Foxp3*$^{YFP\text{-}Cre}$ mice as compared to *Il10*$^{-/-}$ mice (Figure 3C). It seems unlikely that the observed differences were due to distinct flora in mice of different genotypes because they were cohoused and fecal samples from every experimental group tested positive for *H. hepaticus*, *H rodentum* and *H. trogonum* by PCR, whereas *H. bilis* and *H. typhlonus* were not detected. Colitis observed in *Il10*$^{flox/flox}$ × *Foxp3*$^{YFP\text{-}Cre}$ mice was not due to a paucity of Treg cells in the colon; flow-cytometric analysis of the colonic T cell population comprised of both intraepithelial lymphocytes (IEL) and lamina propria lymphocytes (LPL) showed an increased size of the Foxp3^{+} Treg cell subset with unaltered Foxp3 expression on a per-cell basis in *Il10*$^{flox/flox}$ × *Foxp3*$^{YFP\text{-}Cre}$ mice, as compared to the control *Il10*$^{WT/flox}$ × *Foxp3*$^{YFP\text{-}Cre}$ mice (Figure 3D). Thus, IL-10 deficient Treg cells are abundant in the colonic tissue but are unable to restrain inflammation. It was also possible that inability of Foxp3-expressing cells to produce IL-10 in the gut might prevent IL-10 secretion by Foxp3^{-} T cells. To examine this possibility, we isolated LPL from *Il10*$^{flox/flox}$ × *Foxp3*$^{YFP\text{-}Cre}$ and control *Il10*$^{WT/flox}$ ×*Foxp3*$^{YFP\text{-}Cre}$ mice and assessed their ability to produce IL-10 upon in vitro stimulation. IL-10 producing Foxp3^{-} LPL were readily detectable, whereas Foxp3^{+} LPL were lacking (Figure S3B in the Supplemental Data). A moderate, less-than-two-fold reduction in the proportion of IL-10-producing cells could be a result of the inflammatory environment and overall increased T cell infiltration of the tissue. These data together suggest that IL-10 produced by Treg cells plays an important role in restraining local inflammation in the colon.

Heightened Immune-Mediated Lung Hyperreactivity in Il10$^{flox/flox}$ × Foxp3$^{YFP\text{-}Cre}$ Mice

Although the aforementioned histological examination of multiple organs and tissues (heart, skeletal muscle, stomach, pancreas, small intestine, thyroid, and brain) isolated from *Il10*$^{flox/flox}$ × *Foxp3*$^{YFP\text{-}Cre}$ mice did not reveal noticeable pathology, we observed mild perivasculitis and moderate

(B) Southern-blot analysis of DNA isolated from an ES cell clone with the targeted *Foxp3*$^{YFP\text{-}Cre}$ allele. Genomic DNA was digested with *BspHI* restriction enzyme, separated in the agarose gel, and hybridized with a ^{32}P-labeled probe specific for the region indicated in (A). Lane 1, untargeted control ES cell clone; lane 2, targeted ES cell clone used for generation of the knock-in mice.

(C) Flow-cytometric analysis of T cell subsets in *Foxp3*$^{YFP\text{-}Cre}$ mice. Thymocytes, splenocytes, and lymph node cells isolated from 4- to 6-week-old mice were stained for CD4, CD8, CD25, and Foxp3. Twelve mice were analyzed in three independent experiments.

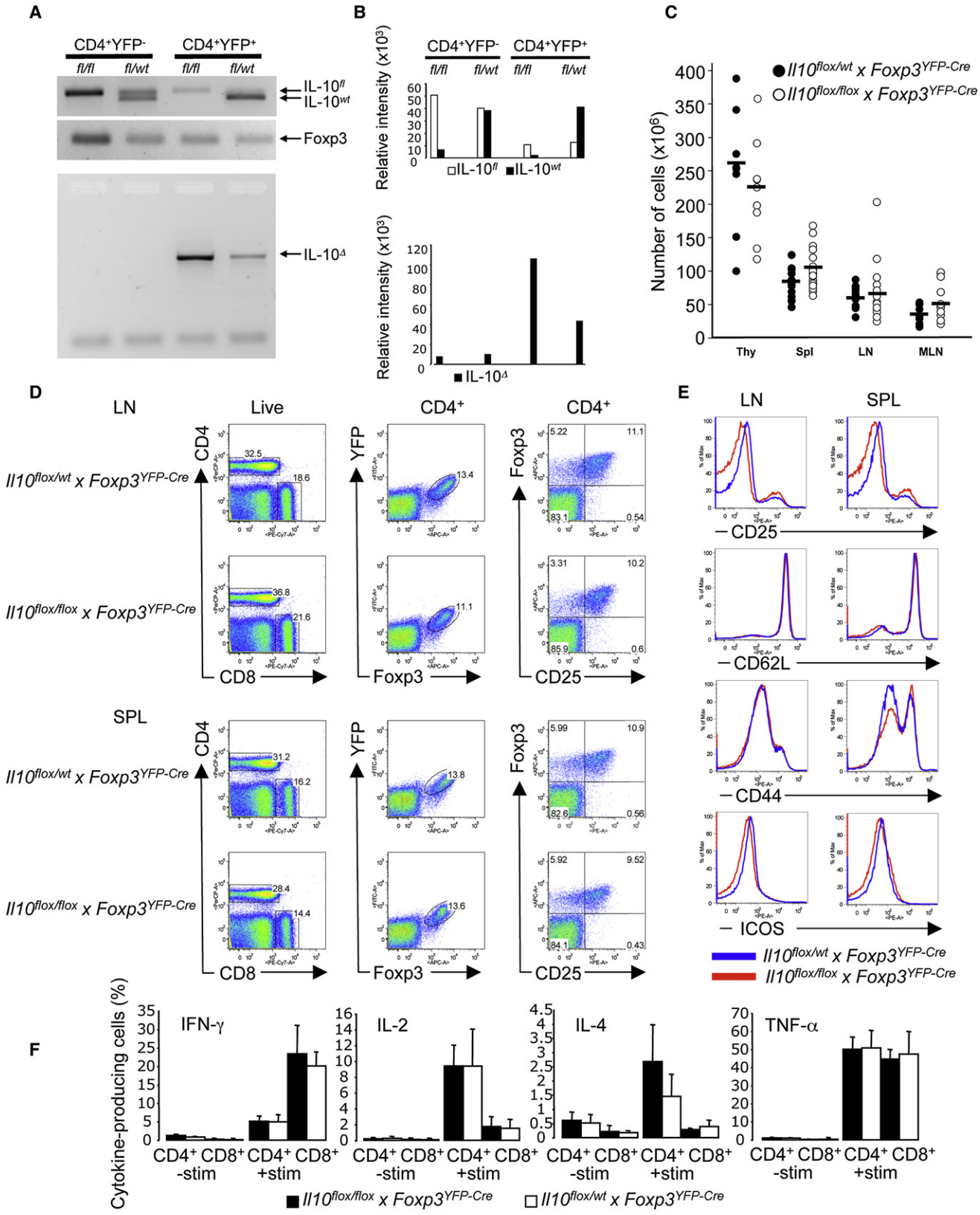

Figure 2. Lack of Systemic Autoimmunity and Normal Development of Treg Cells in Mice with the IL-10 Deficiency Limited to Treg Cells

(A) Deletion of the *Il10* gene in *Il10*$^{flox/flox}$ × *Foxp3*$^{YFP\text{-}Cre}$ mice is restricted to the Foxp3^{+} Treg cell subset. PCR-based analysis of YFP-Cre^{+} and YFP-Cre^{-} CD4^{+} T subsets for the presence of wild-type (*Il10*^{WT}) and conditional undeleted (*Il10*^{flox}) or deleted (*Il10*$^{\Delta}$) *Il10* alleles. Genomic DNA was isolated from the

mononuclear infiltration around large airways in the lungs from *Il10*$^{flox/flox}$ × *Foxp3*$^{YFP\text{-}Cre}$ but not from the littermate control *Il10*$^{WT/flox}$ × *Foxp3*$^{YFP\text{-}Cre}$ mice (Figure 4A). Flow-cytometric analysis of T cell populations isolated from perfused lungs showed an unaltered Foxp3$^+$ T cell subset in *Il10*$^{flox/flox}$ × *Foxp3*$^{YFP\text{-}Cre}$ as compared to *Il10*$^{WT/flox}$ × *Foxp3*$^{YFP\text{-}Cre}$ mice (Figure 4B). Importantly, approximately 12% of Foxp3$^+$ T cells in the lungs express IL-10 based on analysis of IL-10 reporter mice (Maynard and Weaver, personal communication). These initial observations suggested that IL-10 produced by Treg cells might play a role in restraining lung inflammation. However, previous studies utilizing germ-line IL-10-deficient mice in an experimental model of asthma implicated this cytokine in accentuating the lung pathology downstream of the inflammatory reaction. In these experiments, *Il10*$^{-/-}$ mice sensitized with ovalbumin (OVA) presented with greatly diminished airway hyperreactivity despite lung lymphocyte infiltration and eosinophilia comparable to those observed in wild-type mice upon intranasal OVA challenge (Makela et al., 2000). Therefore, we tested the role for IL-10 produced by Treg cells in OVA-induced lung inflammation in *Il10*$^{flox/flox}$ × *Foxp3*$^{YFP\text{-}Cre}$ and in littermate control *Il10*$^{WT/flox}$ × *Foxp3*$^{YFP\text{-}Cre}$ mice. To better account for the potential exacerbation of lung hyperreactivity due to IL-10 deficiency in Treg cells, we utilized the previously described suboptimal regimen of OVA immunization to minimize the induced lung inflammation in the wild-type control group of mice (Henderson et al., 1996; Zhang et al., 1997). Twenty-four hours after the final intranasal challenge, we found augmented inflammation manifested by an approximately 2.7-fold increase in leukocyte numbers in the bronchoalveolar lavage (BAL) fluid recovered from OVA-treated *Il10*$^{flox/flox}$ × *Foxp3*$^{YFP\text{-}Cre}$ as compared to littermate control *Il10*$^{WT/flox}$ × *Foxp3*$^{YFP\text{-}Cre}$ mice (Figure 5A). In addition, histological examination, combined with the morphometry of the lung tissue of the mutant mice, showed markedly increased mucus production, goblet cell expansion, and edema and an increased mass of the cellular infiltrates associated with the increased eosinophilic infiltration around major airways (Figure 5B and Table 1). In agreement with these results, quantitative real-time PCR analysis of lung tissue mRNA isolated from OVA-treated *Il10*$^{flox/flox}$ × *Foxp3*$^{YFP\text{-}Cre}$ animals revealed no marked changes in IL-4 but increased amounts of IL-5, IL-13, and IFN-γ messages when these mice were compared to OVA-sensitized control mice (Figure S4; data not shown). These results were also consistent with the ELISA analysis of the corresponding cytokines in the lung-tissue extracts of OVA-immunized and challenged *Il10*$^{flox/flox}$ × *Foxp3*$^{YFP\text{-}Cre}$ (data not shown). To further evaluate functional consequences of lung inflammation observed by histological means and analyses of BAL cell content, we measured lung resistance by using invasive plethysmography. Consistent with the utilization of the OVA sensitization and challenge protocol for induction of suboptimal lung inflammation in the wild-type mice, neither the OVA- nor the saline-treated *Il10*$^{WT/flox}$ × *Foxp3*$^{YFP\text{-}Cre}$ control mice showed a marked increase in airway hyperreactivity to aerosolized methacholine. However, we found greatly augmented airway hyperreactivity in response to inhaled methacholine in OVA-treated mice but not in saline-treated *Il10*$^{flox/flox}$ × *Foxp3*$^{YFP\text{-}Cre}$ mice (Figure 5C). The increased inflammation in the lungs of the mutant mice was not a consequence of decreased numbers of IL-10-deficient Treg cells in the inflamed lung tissue because increased size of the lung Foxp3$^+$ Treg cell subset was found in mutant OVA-challenged mice (Figure S5). Thus, as in the inflamed colonic tissue, IL-10-deficient Treg cells are present in the lungs in increased numbers; however, they fail to provide complete protection against excessive inflammatory responses initiated by the airborne antigen. Taken together, our data show that IL-10 secretion by Treg cells, in addition to its role in restraining immune-mediated inflammation in the colon, is contributing to Treg cell-mediated suppression of immunological reactivity in the airways.

Increased Skin Hypersensitivity in Il10$^{flox/flox}$ × Foxp3$^{YFP\text{-}Cre}$ Mice

Because we found that the IL-10 production by Treg cells plays a substantial anti-inflammatory role in the lungs and colon, we decided to examine whether immune-mediated inflammation is also affected by the IL-10 deficiency in Treg cells at a third major environmental interface, the skin. Initial examination of skin sections from *Il10*$^{flox/flox}$ × *Foxp3*$^{YFP\text{-}Cre}$ mice failed to reveal noticeable mononuclear infiltration or skin thickening typical of previously described *Foxp3*^{null} mice lacking Treg cells and of *Foxp3*^{DTR} mice subjected to the diphtheria-toxin-mediated Treg cell ablation (Fontenot et al., 2003; Kim et al., 2007). To further explore the question, we sensitized *Il10*$^{flox/flox}$ × *Foxp3*$^{YFP\text{-}Cre}$ and control *Il10*$^{WT/flox}$ × *Foxp3*$^{YFP\text{-}Cre}$ mice by painting the skin at the shaved abdomen region with dinitrofluorobenzene (DNFB) and challenged them by application of DNFB on one ear; the other ear was treated with the vehicle as a control. The

indicated subsets of purified CD4 T cells from *Il10*$^{flox/flox}$ × *Foxp3*$^{YFP\text{-}Cre}$ (*fl/fl*) and *Il10*$^{WT/flox}$ × *Foxp3*$^{YFP\text{-}Cre}$ mice (*fl/wt*) (results of one representative experiment are shown).

(B) Bar graphs show relative intensity of the indicated PCR products normalized to the intensity of the *Foxp3* band used as a control PCR product. The results represent one of two identical experiments.

(C) Cellularity of the thymus and secondary lymphoid organs in 8- to 10-week-old mice is unaffected by the IL-10 ablation in Treg cells. Each symbol represents mononuclear cell number in the thymus (Thy), spleen (Spl), lymph nodes (LN), and colon-draining mesenteric lymph nodes (MLN) in individual *Il10*$^{flox/flox}$ × *Foxp3*$^{YFP\text{-}Cre}$ (open symbols) and *Il10*$^{WT/flox}$ × *Foxp3*$^{YFP\text{-}Cre}$ mice (closed symbols). LN cell counts represent pooled lymph nodes excluding MLN.

(D) Flow-cytometric analysis of splenic and lymph node T cell subsets in *Il10*$^{flox/flox}$ × *Foxp3*$^{YFP\text{-}Cre}$ and *Il10*$^{WT/flox}$ × *Foxp3*$^{YFP\text{-}Cre}$ mice. Twelve mice were analyzed in three independent experiments.

(E) Flow-cytometric analysis of expression of activation markers by splenic and lymph node T cells in 5- to 8-week-old *Il10*$^{flox/flox}$ × *Foxp3*$^{YFP\text{-}Cre}$ and *Il10*$^{WT/flox}$ × *Foxp3*$^{YFP\text{-}Cre}$ mice. Cells were stained for CD4, CD8, CD25, CD62L, and CD44. Gate for YFP$^-$CD4$^+$ cells is shown. Twelve mice were analyzed in three independent experiments.

(F) Analysis of intracellular cytokine expression in total splenocytes stimulated with plate-bound CD3 and CD28 antibodies. Splenocytes were isolated from 6- to 8-week-old *Il10*$^{flox/flox}$ × *Foxp3*$^{YFP\text{-}Cre}$ and *Il10*$^{WT/flox}$ × *Foxp3*$^{YFP\text{-}Cre}$ mice and after 5 hr activation were stained for CD4, CD8, IL-2, IL-4, IFNγ, and TNFα. The data are shown as mean percentages (± standard error) of cytokine-positive cells in CD4$^+$ or CD8$^+$ populations in individual mice. Unstimulated cell samples cultured in the absence of antibodies are shown as a control. Eight animals per group were analyzed in two separate experiments.

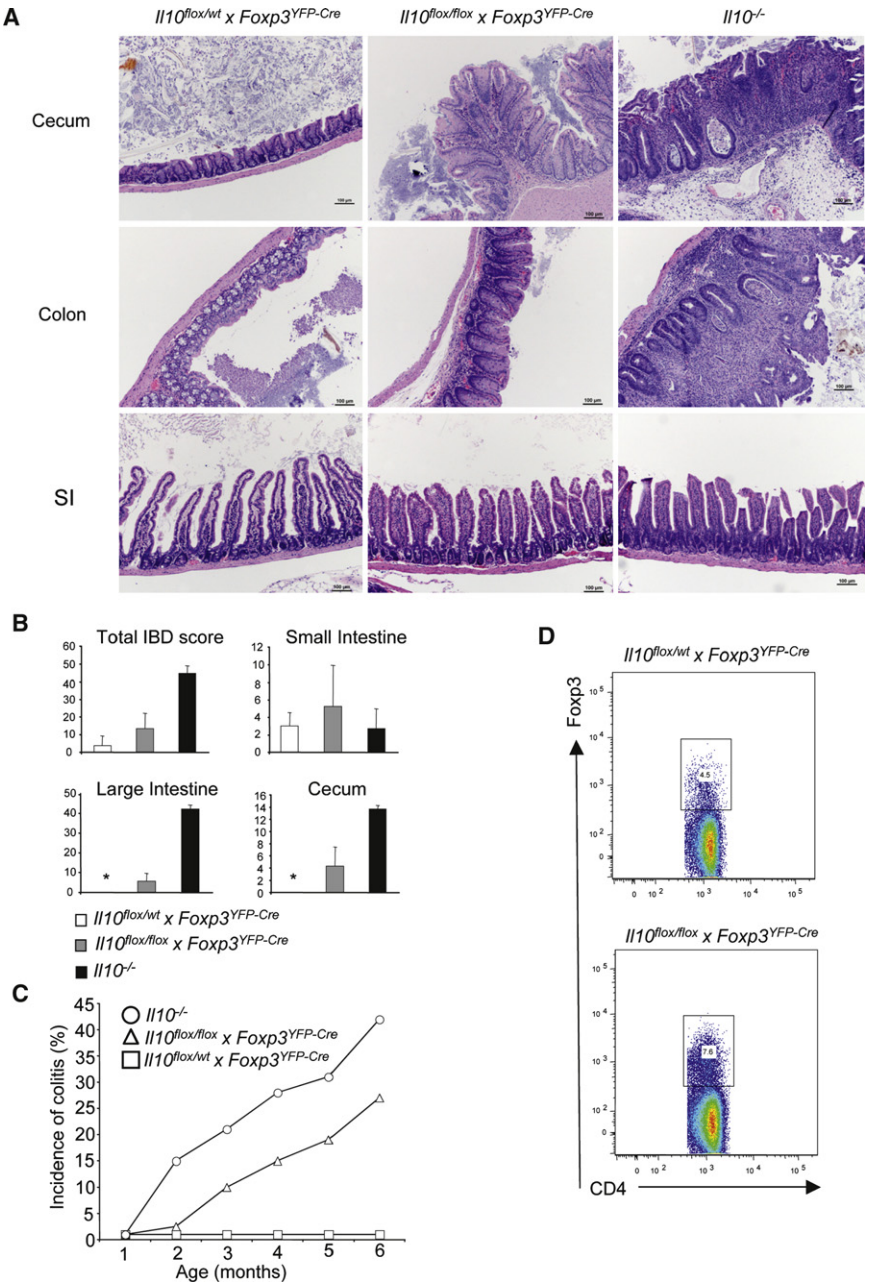

Figure 3. Age-Dependent Spontaneous Colitis in *Il10*$^{flox/flox}$ × *Foxp3*$^{YFP\text{-}Cre}$ Mice

(A) Representative formalin-fixed and hematoxylin- and eosin-stained sections from the cecum (top row), colon (middle row), and small intestines (bottom row) of approximately 3-month-old wild-type, germ-line, and Treg cell-restricted IL-10-deficient mice. The littermate control *Il10*$^{WT/flox}$ × *Foxp3*$^{YFP\text{-}Cre}$ sections are within normal limits (left column). The *Il10*$^{flox/flox}$ × *Foxp3*$^{YFP\text{-}Cre}$ cecum and colon have relatively moderate inflammatory bowel disease-type lesions characterized by mild mucosal hyperplasia and inflammation within the mucosa and submucosa. Compare to the severe lesions characterized by marked mucosal thickening, hyperplasia, glandular loss, crypt abscesses, submucosal edema, and transmural inflammation in the *Il10*$^{-/-}$ mice. In all animals the small-intestinal regions are within normal limits. Original magnification for all images, 10×.

(B) IBD scores of the small and large intestines and cecum of approximately 3-month-old *Il10*$^{flox/flox}$ × *Foxp3*$^{YFP\text{-}Cre}$, littermate control *Il10*$^{WT/flox}$ × *Foxp3*$^{YFP\text{-}Cre}$, and *Il10*$^{-/-}$ mice. Formalin-fixed sections were stained with H&E prior to examination. Mean pathology scores ± standard error are shown; there were 3–6 mice per group.

(C) Incidence of clinical colitis in *Il10*$^{flox/flox}$ × *Foxp3*$^{YFP\text{-}Cre}$ and *Il10*$^{-/-}$ mice. Animals were monitored daily for clinical signs of colitis, including rectal prolapse and diarrhea. Colitis was further confirmed by macroscopic examination of the colon and selective tissue histopathology. Number of animals in each cohort: *Il10*$^{flox/flox}$ × *Foxp3*$^{YFP\text{-}Cre}$, 140; *Il10*$^{WT/flox}$ × *Foxp3*$^{YFP\text{-}Cre}$, 128; and *Il10*$^{-/-}$, 42.

(D) Flow-cytometric analysis of colonic Foxp3$^+$ Treg cells in *Il10*$^{flox/flox}$ × *Foxp3*$^{YFP\text{-}Cre}$ mice. Colonic IEL and LPL were isolated from three mice of each indicated genotype, pooled, and stained for CD4, CD8, TCRβ, and Foxp3. Gate for CD4$^+$CD8$^-$TCRβ$^+$ cells is shown. A representative of two independent experiments is shown.

ensuing skin hypersensitivity reaction was assessed by ear thickness measured before and after the challenge. We found a substantial increase in ear thickness and heightened inflammation in *Il10*$^{flox/flox}$ × *Foxp3*$^{YFP\text{-}Cre}$ mice as compared to the control animals (Figures 6A and 6B). To examine whether the increased skin hypersensitivity in *Il10*$^{flox/flox}$ × *Foxp3*$^{YFP\text{-}Cre}$ mice was due to Treg cell homing deficiency, i.e., the inability to home to the skin, or due to their impaired suppressor capacity, we examined CD4$^+$ T cell subsets in the ears of the mutant mice. As in analogous analyses of lung and colon tissue, we found the same proportion of the FoxP3$^+$ CD4$^+$ T cells in the skin of mutant and control mice (Figure 6C). It is noteworthy that the expression of the T cell activation marker CD69 on non-Treg cells was higher in mutant mice than in control mice (data not shown). Thus, Treg cells lacking IL-10 production are not as effective in controlling inflammation in skin as their IL-10-sufficient counterparts. Together, our studies suggest that the production of IL-10 by Treg cells is limiting inflammation at environmental interfaces and is at the same time dispensable for control of systemic autoimmunity.

DISCUSSION

Foxp3-expressing Treg cells play a central role in immunological tolerance to self and environmental antigens and in limiting tissue damage associated with the immune response to pathogens. Recent reports have suggested that Treg cells are capable of controlling the activation of a variety of immune cell types, including CD4$^+$ and CD8$^+$ T cells, B cells, NK cells, dendritic cells,

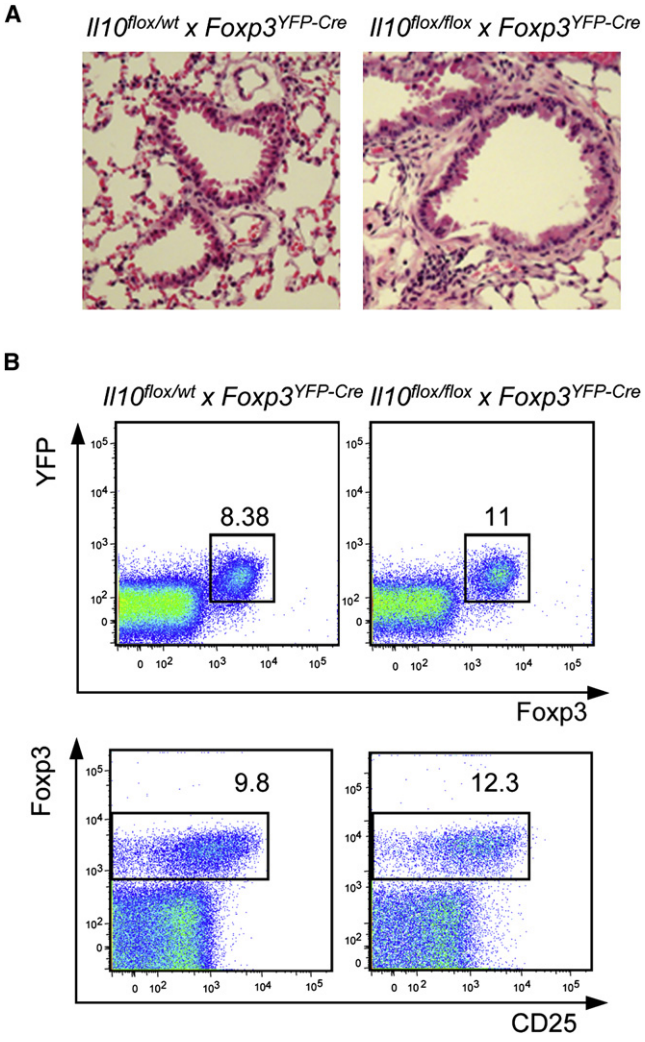

Figure 4. Minor Peribronchial Inflammation and a Normal Size of the Foxp3$^+$ Treg Cell Subset in the Lungs of Unmanipulated *Il10*$^{flox/flox}$ × *Foxp3*$^{YFP\text{-}Cre}$ Mice

(A) Histology sections of lungs from mice with a Treg cell-restricted IL-10 deficiency. Formalin-fixed sections of lungs of approximately 3-month-old *Il10*$^{flox/flox}$ × *Foxp3*$^{YFP\text{-}Cre}$ and littermate control *Il10*$^{WT/flox}$ × *Foxp3*$^{YFP\text{-}Cre}$ mice were stained with H&E. Original magnification, 10×.

(B) Flow-cytometric analysis of Foxp3$^+$ Treg cells in the lung tissue of *Il10*$^{flox/flox}$ × *Foxp3*$^{YFP\text{-}Cre}$ and littermate control *Il10*$^{WT/flox}$ × *Foxp3*$^{YFP\text{-}Cre}$ mice. A lung-resident population of mononuclear cells was isolated from PBS-perfused lungs. Cells isolated from three mice of each genotype were pooled and stained for CD4, CD8, CD25, and Foxp3. The CD4$^+$CD8$^-$ T cell gate is shown. A representative of two identical experiments is shown.

and macrophages. Furthermore, numerous mechanisms were proposed to be responsible for Treg cell-mediated suppression; these included production of immunomodulatory cytokines IL-10 and TGF-β (Asseman et al., 1999; Chen et al., 2005), CTLA-4-mediated cross-linking of B7 molecules on the surface of activated T cells or APC (Oderup et al., 2006; Paust et al., 2004; Tang et al., 2004), elaboration of extracellular adenosine through the cooperative action of ectonucleotidases CD39 and CD73 (Deaglio et al., 2007), extrusion of cAMP (Bopp et al., 2007), and cytolytic activity mediated by granzymes (Gondek et al., 2005) as well as several additional hypothetical mechanisms (Mahic et al., 2006). However, an unequivocal proof of a unique or non-redundant role for any of the above mechanisms in regulatory T cell-mediated suppression in un-manipulated mice has been lacking.

Recent studies have established that the suppressor function of regulatory T cells is critically dependent upon expression of the Foxp3 protein. This conclusion is supported by a loss of suppressor function by genetically marked T cells transcribing the *Foxp3* locus yet lacking in functional Foxp3 protein expression in mice with the targeted insertion of GFP into the Foxp3 locus (Gavin et al., 2007; Lin et al., 2007). Furthermore, a decreased Foxp3 protein expression in Treg cells as a result of induced dysregulation of *Foxp3* gene transcription resulted in a marked attenuation of the suppressor function (Wan and Flavell, 2007). In agreement with these results, the Foxp3 ablation in mature Treg cells through the Cre-mediated deletion of a conditional *Foxp3* allele results in a loss of suppressor function (Williams and Rudensky, 2007). Genome-wide analyses of Foxp3 binding sites utilizing ex vivo-isolated mouse Treg cells or the Foxp3 transfected hybridoma cell line revealed a relatively small number of directly Foxp3-regulated genes, including few genes encoding putative effector molecules, e.g., CTLA4 and Nt5e (Marson et al., 2007; Zheng et al., 2007). In light of these results, it is reasonable to speculate that Foxp3 induces expression of a unique gene mediating suppressor function of Treg cells. Mice lacking such a gene are expected to develop a rapid and fatal autoimmune syndrome analogous to that described in *Foxp3*^{DTR} mice subjected to chronic Treg cell ablation (Kim et al., 2007). Alternatively, it is possible that Treg cells employ multiple immunomodulatory or suppressive molecules, not necessarily unique to Treg cells, that are employed by these cells with a great deal of efficiency as a result of a superior proliferative and metabolic potential, as well as a migratory capacity bestowed by Foxp3 (Gavin et al., 2002; Gavin et al., 2007; Kim et al., 2007; Komatsu and Hori, 2007; Zheng et al., 2007). It is reasonable to speculate that a given suppressive mechanism might operate in a particular inflammatory-tissue setting. A corollary to this scenario is that spontaneous inflammatory lesions resulting from a deficiency in a single effector mechanism will be much less severe and pervasive than those resulting from a lack of the entire Treg cell subset.

As discussed above, pioneering studies by Powrie and coworkers implicated IL-10 in Treg cell-mediated suppression of induction of immune-mediated colitis. These studies relied on adoptive T cell transfer into lymphopenic hosts and antibody-mediated neutralization of IL-10 or IL-10R (Annacker et al., 2003; Asseman et al., 1999; Asseman et al., 2003; Singh et al., 2001). Furthermore, provision of IL-10-sufficient but not IL-10-deficient CD25$^+$CD4$^+$ T cells resolves the established intestinal inflammation (Uhlig et al., 2006). A priori IL-10 cannot be a unique suppressor molecule utilized by Treg cells. Within the immune system, multiple cell types, including B cells, T cells, mast cells, and dendritic cells, produce IL-10 (Moore et al., 2001). Functional significance of IL-10 production by diverse cell types was highlighted by recent observations of an important role for mast cell-derived IL-10 in cutaneous hypersensitivity reactions induced upon immunization or chronic UV irradiation (Grimbaldeston et al., 2007). The germ-line deletion of the *Il10* gene

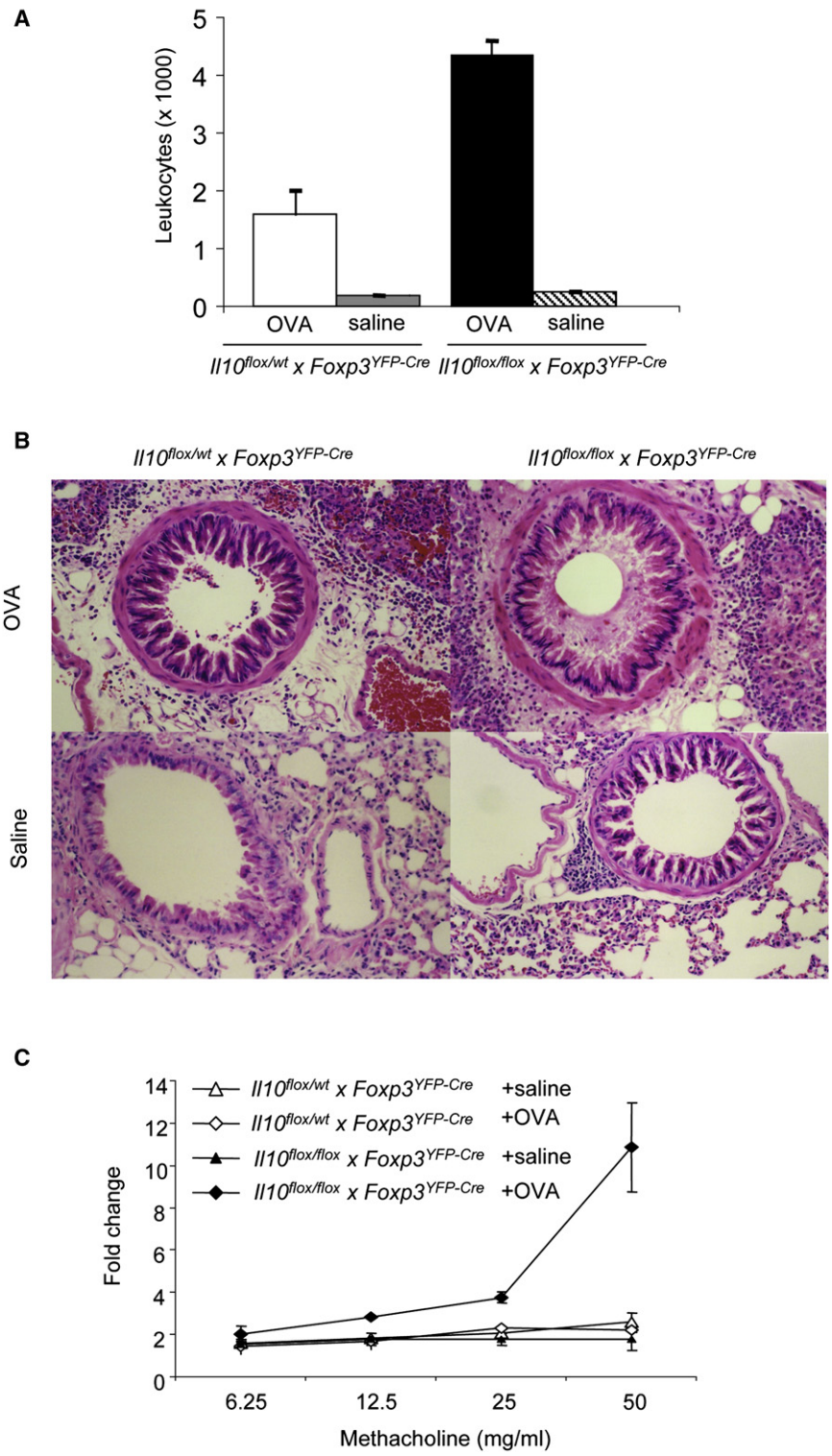

Figure 5. Increased Lung Allergic Inflammation and Hyperreactivity in *Il10*$^{flox/flox}$ × *Foxp3*$^{YFP\text{-}Cre}$ Mice

(A) Increased number of leukocytes in BAL fluid of OVA primed *Il10*$^{flox/flox}$ × *Foxp3*$^{YFP\text{-}Cre}$ mice induced upon OVA or saline (control) challenge. Cellular composition of BAL fluid was examined as described in the Experimental Procedures. The data represent mean BAL leukocyte number ± standard error (n = 8 per group in each of three independent experiments).

(B) Histopathology of lungs isolated from OVA-challenged *Il10*$^{flox/flox}$ × *Foxp3*$^{YFP\text{-}Cre}$ and littermate control *Il10*$^{WT/flox}$ × *Foxp3*$^{YFP\text{-}Cre}$ mice. Mice primed with OVA or saline (control) were rechallenged upon intranasal administration of OVA or saline. A representative of five mice per group from three independent experiments is shown. Original magnification, 40×.

(C) Augmented lung resistance in OVA-challenged *Il10*$^{flox/flox}$ × *Foxp3*$^{YFP\text{-}Cre}$ mice. Methacholine-induced lung resistance was measured via invasive plethysmography in OVA-challenged *Il10*$^{flox/flox}$ × *Foxp3*$^{YFP\text{-}Cre}$ and littermate control *Il10*$^{WT/flox}$ × *Foxp3*$^{YFP\text{-}Cre}$ mice (n = 4–5 per group). The data are shown as the mean n-fold change of R_L values (± standard error) as compared to mice not treated with methacholine. A representative of three independent experiments is shown.

leads to fulminant spontaneous colitis but not to the fatal and rapid disease observed in Foxp3 mutant mice (Berg et al., 1995; Fontenot et al., 2003; Kuhn et al., 1993). Importantly, we previously reported that the ablation of the *Il10* gene in T cell lineage results in a comparably severe colitis, increased skin hypersensitivity, and the fatal immunopathology associated with *Toxoplasma gondii* infection (Roers et al., 2004). However, within the T cell lineage, multiple T cell subsets other than Treg cells, including NKT cells, Foxp3$^-$ Tr1 cells, and conventional IFN-γ-producing effector CD4$^+$ T cells elicited in the course of immune response to a pathogen such as *Toxoplasma gondii* or *Leishmania major,* can serve as a major source of IL-10 production (Anderson et al., 2007; Jankovic et al., 2007; Nylen et al., 2007; Roers et al., 2004). Therefore, elucidation of a functional significance of IL-10 production by Treg cells in control of immune inflammation in unmanipulated mice should provide an acid test for the aforementioned opposing models of Treg cell-mediated suppression.

Here, through the ablation of a conditional *Il10* allele in Treg cells, and using Cre recombinase knocked into the 3′ UTR of the *Foxp3* locus, we found that IL-10 plays a prominent role in Treg cell suppressive function in the colon, lung, and skin. Consistent with the recent findings that some IL-10-expressing T cells in the colonic lamina propria (and the majority of these cells in the small intestine) do not express Foxp3, spontaneous intestinal inflammation was largely limited to the colon, and its severity was less pronounced in *Foxp3*$^{YFP\text{-}Cre}$ mice than in mice with the germ-line or T cell-specific IL-10 deficiency

Table 1. Morphometric Analysis of Antigen-Induced Lung Inflammation in *IL10* × *Foxp3*$^{YFP\text{-}Cre}$ Mice

	Il10$^{WT/flox}$ × *Foxp3*$^{YFP\text{-}Cre}$		*Il10*$^{flox/flox}$ × *Foxp3*$^{YFP\text{-}Cre}$	
Lung Pathology Score	Saline/Saline	OVA/OVA	Saline/Saline	OVA/OVA
Total Inflammatory Cell Infiltrate in Lungs (0–4+)	0.0 ± 0.0	2.3 ± 0.3	0.05 ± 0.05	3.7 ± 0.3[a]
Eosinophil infiltrate (eosinophils/unit of lung tissue area)	0.1 ± 0.1	15.9 ± 0.1	0.25 ± 0.19	23.4 ± 2.4[a]
Mucus occlusion of airway diameter (0–4+)	0.1 ± 0.06	2.4 ± 0.1	0.05 ± 0.05	3.7 ± 0.2[a]
Goblet cells (percent of airway epithelial cells)	0.1 ± 0.06	24.0 ± 4.2	0.05 ± 0.05	38.7 ± 5.3[a]
Airway edema (0–4+)	0.1 ± 0.06	1.4 ± 0.2	0.05 ± 0.05	2.4 ± 0.3[a]

Ten sections per mouse were evaluated on a 0–4+ scale. The data are presented as the mean score (± standard error). Eight to ten mice per group were analyzed in two independent experiments.
[a] p values of the differences between mean scores for OVA-treated *Il10*$^{flox/flox}$ × *Foxp3*$^{YFP\text{-}Cre}$ and *Il10*$^{WT/flox}$ × *Foxp3*$^{YFP\text{-}Cre}$ mice were between 0.0001 and 0.0156.

(Kamanaka et al., 2006; Maynard et al., 2007; Roers et al., 2004). In contrast to spontaneous colonic inflammation, unchallenged *Il10*$^{flox/flox}$ × *Foxp3*$^{YFP\text{-}Cre}$ mice maintained under SPF conditions showed very little immune-mediated inflammation in the skin or lungs (data not shown). Nevertheless, upon induction of local antigen-specific immune responses, a markedly enhanced inflammation and tissue pathology was observed in the absence of Treg cell-derived IL-10 in the experimental models of the skin and lung hypersensitivity. Interestingly, in contrast to a sharp increase in airway resistance in OVA-challenged *Il10*$^{flox/flox}$ × *Foxp3*$^{YFP\text{-}Cre}$ mice, the airway resistance was not markedly augmented in *Il10*$^{-/-}$ mice in comparison to wild-type mice (data not shown). The latter observation is in agreement with another study of *Il10*$^{-/-}$ mice (Makela et al., 2000); this study also utilized OVA-induced lung inflammation. Lack of lung hyper-reactivity in *Il10*$^{-/-}$ mice can be explained by previously proposed regulation of smooth-muscle contraction by IL-10 originating from cells other than Treg cells (Makela et al., 2000). In addition, it is possible that a more prominent profuse colitis in mice with the germline IL-10 deficiency than in mice in which the IL-10 deficiency limited to Treg cells results in a massive focus of intestinal inflammation, "detracting" pro-inflammatory cells from the lung. We further speculate that this observation of "immune detraction" in the model of induced lung hypersensitivity might be applicable to other types of immune inflammation.

It is noteworthy that the acquisition of IL-10 production by Treg cells, a particular, functionally important suppressor modality, is likely to be facilitated by the environment at mucosal interfaces. This notion comes from the observations that despite the fact that IL-10 expression can be found in a subset of Foxp3^{+} Treg cells present in tissues such as colon or lung, Foxp3-expressing thymocytes lack IL-10 expression.

Our studies demonstrate that IL-10 produced by Treg cells is not required for limiting systemic autoimmunity but is needed for restraining immunological hyperreactivity at environmental interfaces. In contrast, CTLA-4 ablation in Treg cells resulted in systemic lymphoproliferative syndrome and severe pancreatic lesions, whereas the colon and skin remained largely unaffected (Y.P.R., A. Paterson, A. Sharpe, and A.Y.R., unpublished observations). These results strongly suggest that Treg cells utilize multiple means to limit the immune response and that suppressive mechanisms utilized by Treg cells are likely to be nonredundant, or only partially redundant, with individual suppressor mechanisms operating in a particular tissue and inflammatory setting.

EXPERIMENTAL PROCEDURES

Mice

Il10$^{flox/flox}$ mice have been described elsewhere (Roers et al., 2004). *Il10*$^{-/-}$ animals were purchased from the Jackson Laboratory. *Il10*$^{flox/flox}$ mice were on the C57BL/6 background, whereas *Foxp3*$^{YFP\text{-}Cre}$ mice, originally on a mixed B6/129 background, were backcrossed onto the C57BL/6J background three to four times in the process of generating *Il10*$^{flox/flox}$ × *Foxp3*$^{YFP\text{-}Cre}$ mice. All mice were maintained in the University of Washington specific pathogen-free facility that was *Helicobacter* species positive and handled in accordance with the institutional guidelines for animal care and use.

Generation of the Targeted Foxp3$^{YFP\text{-}Cre}$ Allele

A 7.9 kilobase (kb) XbaI fragment of the *Foxp3* locus containing exons 6 through 11 was subcloned from a 30.8 kb cosmid containing the complete Foxp3 gene into a pBluescript vector containing a PGK-DTA-negative selection cassette. A SalI restriction site was engineered in place of the BaeI site present in the 3′ UTR region of the *Foxp3* gene, upstream of the polyadenylation signal. To generate the targeting construct, we cloned IRES-YFP-Cre-BGHpA-FRT-Neo-FRT cassette provided by Richard Locksley (UCSF) into the SalI site. The linearized targeting construct was electroporated into R1 ES cells, and neomycin-resistant clones were screened by PCR across the 3′ arm for evidence of the homologous recombination. Positive clones were further screened by Southern blot analysis of BspHI-digested genomic DNA. ES cell clones harboring the correctly targeted *Foxp3* locus were injected into C57BL/6 blastocysts, and chimeric male offspring were mated to the FLP-deleter transgenic strain of mice so that the PGK-Neo cassette would be excised. Germ-line transmission of the targeted allele was confirmed by PCR with genomic tail DNA.

PCR Confirmation of the Deletion of the Il10flox Allele

Genomic DNA from sorted T cells was isolated with DNeasy Blood & Tissue Kit (QIAGEN) and diluted to a final concentration 5 ng/μl in Tris-EDTA buffer (pH 7.4). Serial dilutions of template were used in PCR with two pairs of *Il10*-specific primers: 5′-ACTGGCTCAGCACTGCTATGC-3′ and 5′-GCCTTCTTTGGACCTCCATACCAG-3′ for detecting *Il10*^{flox} or *Il10*^{wt} alleles; 5′-CAGGATTTGACAGTGCTAGAGC-3 and 5′-AAACCCAGCTCAAATCTCCTGC-3′ for detecting the *Il10* allele lacking excised floxed fragment. To normalize the amount of input DNA, we used PCR with primers to the *Foxp3* gene: 5′-AGACAGACCAGAGGTGTAGT-3′ and 5′-TCCTGGGGATGGGCCAAGGGCCAAGG-3′.

Preparation of Single-Cell Lymphocyte Suspensions from the Lung, Colon, and Skin

Prior to collection, lungs were perfused with 10 ml PBS and minced with scissors. After addition of 10 ml DMEM, 5% FCS, collagenase D (Roche, 2 mg/ml), and DNase (30 μg/ml), tissue fragments were incubated at 37°C for 30 min in an orbital shaker, collected by centrifugation, resuspended in HBSS, 5 mM EDTA, and 5% FCS for 5 min at 37°C with shaking, and filtered through a 100 μm cell strainer. Cells were washed twice with PBS and subjected to flow-cytometric analysis. Lymphocyte-containing cell suspension from the total colon was prepared according to a modified protocol (Drakes et al.,

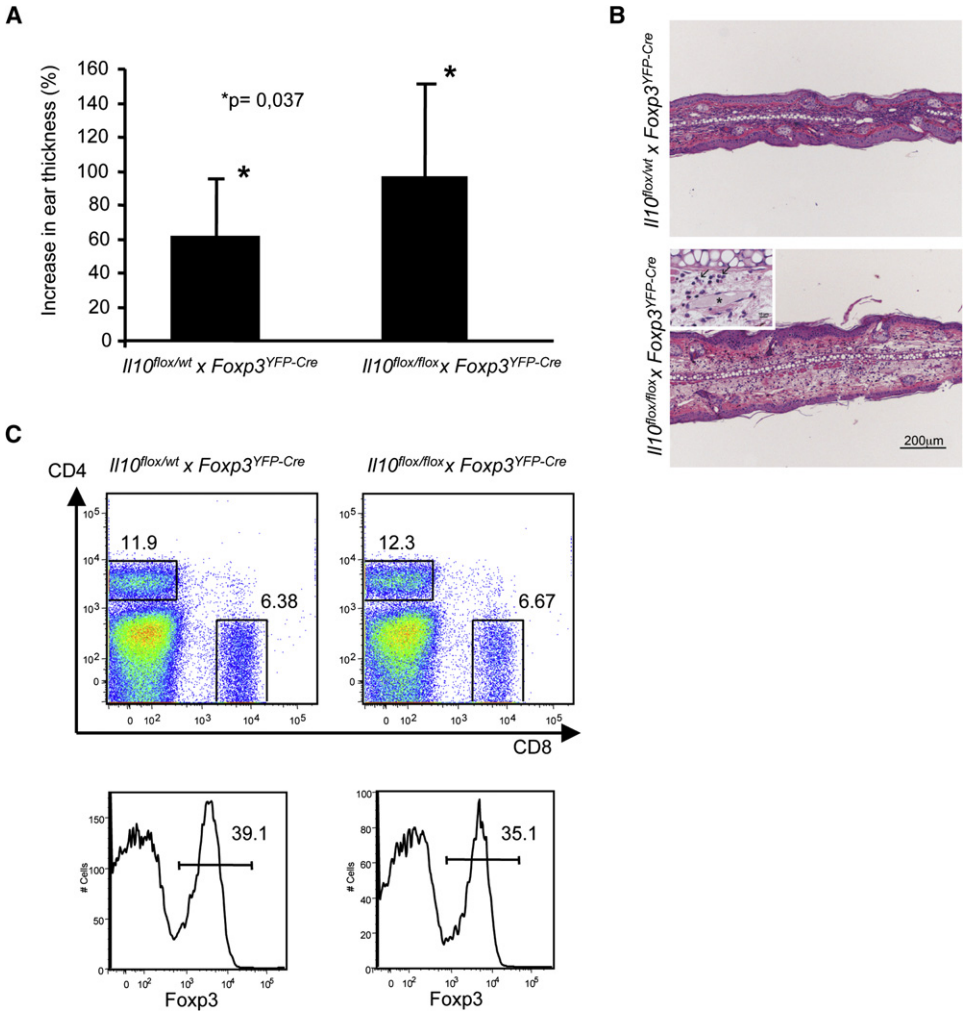

Figure 6. Increased Contact Hypersensitivity Reaction in *Il10*$^{flox/flox}$ × *Foxp3*$^{YFP\text{-}Cre}$ Mice

(A) Increased ear thickness in *Il10*$^{flox/flox}$ × *Foxp3*$^{YFP\text{-}Cre}$ mice as compared with *Il10*$^{WT/flox}$ × *Foxp3*$^{YFP\text{-}Cre}$ littermate controls 48 hr after challenge with DNFB. Ear thickness was measured with a caliper prior to and 48 hr after antigenic challenge. The data are shown as the percent increase in ear thickness compared to thickness of the same ear before it was painted with DNFB. Twelve mice were used per group in each of two independent experiments.

(B) Histology sections of skin (ears) challenged with DNFB so that a skin-contact hypersensitivity reaction would be induced in sensitized littermate control *Il10*$^{WT/flox}$ × *Foxp3*$^{YFP\text{-}Cre}$ and *Il10*$^{flox/flox}$ × *Foxp3*$^{YFP\text{-}Cre}$ mice. Formalin-fixed sections stained with hematoxylin and eosin from the same region of the pinnae are presented. Note marked subcutaneous expansion of the *Il10*$^{flox/flox}$ × *Foxp3*$^{YFP\text{-}Cre}$ pinnae by edema with inflammatory cells. Original magnification, 10×. Inset: higher magnification of *Il10*$^{flox/flox}$ × *Foxp3*$^{YFP\text{-}Cre}$. Note dilated lymphatic and inflammatory cells (arrows) next to a smooth-muscle cell (asterix). Original magnification, 60×.

(C) Frequency of Foxp3^{+} Treg cells in the skin at the site of antigenic challenge is not changed in *Il10*$^{flox/flox}$ × *Foxp3*$^{YFP\text{-}Cre}$ mice as compared to littermate controls. Flow-cytometric analysis of skin T cell subsets isolated from the DNFB-painted ears of *Il10*$^{flox/flox}$ × *Foxp3*$^{YFP\text{-}Cre}$ and *Il10*$^{WT/flox}$ × *Foxp3*$^{YFP\text{-}Cre}$ mice. Expression of Foxp3 in the CD4^{+}CD8^{-} T cell gate is shown.

2005). Lymphocyte-containing cell populations were isolated from the ear skin as described (Ohl et al., 2004).

Cell Purification and Flow-Cytometric Analysis of T Cell Subsets and Cytokine Production

Cell populations were purified with magnetic beads and an AutoMACS magnetic cell sorter (Miltenyi Biotec) or with a FACSAria fluorescent cell sorter (BD Biosciences). The purity of all cell preparations was >90%. Flow-cytometric analyses were carried out with a FACSCanto flow cytometer (BD Biosciences). Fluorochrome-conjugated mouse CD4, CD8a, CD44, CD69, CD62L, CD25, and Foxp3 antibodies (BD Biosciences or eBioscience) were used. Flow-cytometric analysis of cytokine production was performed as described elsewhere (Williams and Rudensky, 2007). For IL-10 secretion analysis, cells were plated in round-bottom plates at 5 × 10^{5}/ml in 0.2 ml of RPMI/10% FCS. LPL cells were stimulated in vitro with PMA (100 ng/ml) and ionomycin (1 μg/ml) for 4 hr in the presence of Golgi Plug (BD PharMingen). Splenocytes were stimulated with plate-bound CD3 and CD28 antibodies (1 μg/ml each) for 72 hr in the presence of rhTGF-β1 (2 ng/ml) and IL-2 (100 U/ml) and restimulated for 4 hr with PMA and ionomycin (50 ng/ml and 500 ng/ml, respectively) in the presence of Golgi Plug. Stimulated and unstimulated control cells were stained for surface expression of CD4, FoxP3, and IL-10 antibodies according to the manufacturer's (eBioscience's) protocol.

Histopathological Evaluation of Spontaneous Colitis

Samples of small intestine, cecum, and colon from 3–4 animals per group were fixed in 10% neutral buffered formalin and processed routinely for hematoxylin

and eosin staining. Histological evaluation of colitis within the cecum and proximal and mid-colon was performed as described previously (Burich et al., 2001), except that the small intestine was included. In brief, a pathologist blinded to genotype and using a 0–4 scale scored mucosal changes (erosion, ulceration, and/or hyperplasia), inflammation, and extent of section involvement. An inflammatory bowel disease (IBD) score was generated from the sum of the individual section scores.

Induction of Allergic Lung Inflammation and Evaluation of Lung Function and Lung Histopathology

Mice received two i.p. injections of 100 μg OVA (Pierce Chemical Co.) complexed with aluminum potassium sulfate (alum; Sigma-Aldrich) in 0.2 ml on days 1 and 14. Mice were anesthetized by administration of 130 mg/kg ketamine and 8.8 mg/kg xylazine in saline prior to intranasal (i.n.) challenge with 100 μg OVA (0.05 ml; 2 mg/ml) on day 14 and with 50 μg OVA (0.05 ml; 1 mg/ml) on day 25 (Henderson et al., 1996; Zhang et al., 1997). Control groups of mice received 0.2 ml saline with alum i.p. on days 1 and 14 and 0.05 ml saline without alum i.n. on days 14 and 25. For BAL cell isolation, the right lung was lavaged three times with 0.5 ml of normal saline 24 hr after the final OVA or saline treatment, and cells were analyzed as described (Henderson et al., 1996).

To evaluate pulmonary function, we measured invasive pulmonary mechanics in mice in response to methacholine as previously described (Henderson et al., 2007; Henderson et al., 1996), except the thorax was not opened. Lung pathology evaluation was performed in a blinded fashion as described elsewhere (Henderson et al., 2005) (for a detailed description, see Supplemental Data).

Real-Time PCR

Total RNA was isolated from the right lung with an RNeasy mini kit (QIAGEN), and mRNA amounts for IL-4, IL-5, IL-13, IFN-γ, and GAPDH were determined by quantitative PCR on a 7900HT instrument (Applied Biosystems). For design of all primers, Primer 3 software was used across the intronic sequences (Table S1). PCR product sizes of ~100 bp were confirmed by gel electrophoresis.

Skin-Contact Hypersensitivity Reaction

We induced skin hypersensitivity by painting the shaved abdomen with 100 μl 0.5% (wt/vol) dinitrofluorobenzene (DNFB; Sigma-Aldrich) in a 4:1 mixture of acetone and olive oil for sensitization. The mice were challenged 6 days later by application of 10 μl 0.2% (wt/vol) DNFB in olive oil to each side of one ear. Ear thickness was determined with an engineer's caliper (Mitutoyo) before challenge and at 48 hr after treatment. The percent increase of ear thickness was compared for the different experimental groups with the Student's t test for independent samples (Roers et al., 2004). We performed routine formalin fixation and processing on selected animals to characterize the histopathological lesions.

SUPPLEMENTAL DATA

One table, five figures, and additional Experimental Procedures are available online at http://www.immunity.com/cgi/content/full/28/4/546/DC1/.

ACKNOWLEDGMENTS

We thank C. Maynard and C. Weaver (University of Alabama-Birmingham) for sharing unpublished data; D. Liggitt for assistance with the analysis of histopathology; K. Forbush, L. Karpik, and T. Chu for assistance, and members of the Rudensky lab for discussions. This work was supported by the Howard Hughes Medical Institute (A.Y.R.) and US National Institutes of Health (A.Y.R. and W.R.H.).

Received: September 21, 2007
Revised: January 11, 2008
Accepted: February 13, 2008
Published online: April 3, 2008

REFERENCES

Anderson, C.F., Oukka, M., Kuchroo, V.J., and Sacks, D. (2007). CD4(+)CD25(-)Foxp3(-) Th1 cells are the source of IL-10-mediated immune suppression in chronic cutaneous leishmaniasis. J. Exp. Med. *204*, 285–297.

Annacker, O., Asseman, C., Read, S., and Powrie, F. (2003). Interleukin-10 in the regulation of T cell-induced colitis. J. Autoimmun. *20*, 277–279.

Asseman, C., Mauze, S., Leach, M.W., Coffman, R.L., and Powrie, F. (1999). An essential role for interleukin 10 in the function of regulatory T cells that inhibit intestinal inflammation. J. Exp. Med. *190*, 995–1004.

Asseman, C., Read, S., and Powrie, F. (2003). Colitogenic Th1 cells are present in the antigen-experienced T cell pool in normal mice: control by CD4+ regulatory T cells and IL-10. J. Immunol. *171*, 971–978.

Berg, D.J., Leach, M.W., Kuhn, R., Rajewsky, K., Muller, W., Davidson, N.J., and Rennick, D. (1995). Interleukin 10 but not interleukin 4 is a natural suppressant of cutaneous inflammatory responses. J. Exp. Med. *182*, 99–108.

Bopp, T., Becker, C., Klein, M., Klein-Hessling, S., Palmetshofer, A., Serfling, E., Heib, V., Becker, M., Kubach, J., Schmitt, S., et al. (2007). Cyclic adenosine monophosphate is a key component of regulatory T cell-mediated suppression. J. Exp. Med. *204*, 1303–1310.

Brunkow, M.E., Jeffery, E.W., Hjerrild, K.A., Paeper, B., Clark, L.B., Yasayko, S.A., Wilkinson, J.E., Galas, D., Ziegler, S.F., and Ramsdell, F. (2001). Disruption of a new forkhead/winged-helix protein, scurfin, results in the fatal lymphoproliferative disorder of the scurfy mouse. Nat. Genet. *27*, 68–73.

Burich, A., Hershberg, R., Waggie, K., Zeng, W., Brabb, T., Westrich, G., Viney, J.L., and Maggio-Price, L. (2001). Helicobacter-induced inflammatory bowel disease in IL-10- and T cell- deficient mice. Am. J. Physiol. Gastrointest. Liver Physiol. *281*, G764–G778.

Chen, M.L., Pittet, M.J., Gorelik, L., Flavell, R.A., Weissleder, R., von Boehmer, H., and Khazaie, K. (2005). Regulatory T cells suppress tumor-specific CD8 T cell cytotoxicity through TGF-beta signals in vivo. Proc. Natl. Acad. Sci. USA *102*, 419–424.

Deaglio, S., Dwyer, K.M., Gao, W., Friedman, D., Usheva, A., Erat, A., Chen, J.F., Enjyoji, K., Linden, J., Oukka, M., et al. (2007). Adenosine generation catalyzed by CD39 and CD73 expressed on regulatory T cells mediates immune suppression. J. Exp. Med. *204*, 1257–1265.

Drakes, M.L., Blanchard, T.G., and Czinn, S.J. (2005). Colon lamina propria dendritic cells induce a proinflammatory cytokine response in lamina propria T cells in the SCID mouse model of colitis. J. Leukoc. Biol. *78*, 1291–1300.

Fahlen, L., Read, S., Gorelik, L., Hurst, S.D., Coffman, R.L., Flavell, R.A., and Powrie, F. (2005). T cells that cannot respond to TGF-beta escape control by CD4(+)CD25(+) regulatory T cells. J. Exp. Med. *201*, 737–746.

Fontenot, J.D., Gavin, M.A., and Rudensky, A.Y. (2003). Foxp3 programs the development and function of CD4+CD25+ regulatory T cells. Nat. Immunol. *4*, 330–336.

Fontenot, J.D., Rasmussen, J.P., Williams, L.M., Dooley, J.L., Farr, A.G., and Rudensky, A.Y. (2005). Regulatory T cell lineage specification by the forkhead transcription factor foxp3. Immunity *22*, 329–341.

Fontenot, J.D., and Rudensky, A.Y. (2005). A well adapted regulatory contrivance: regulatory T cell development and the forkhead family transcription factor Foxp3. Nat. Immunol. *6*, 331–337.

Gavin, M.A., Clarke, S.R., Negrou, E., Gallegos, A., and Rudensky, A. (2002). Homeostasis and anergy of CD4(+)CD25(+) suppressor T cells in vivo. Nat. Immunol. *3*, 33–41.

Gavin, M.A., Rasmussen, J.P., Fontenot, J.D., Vasta, V., Manganiello, V.C., Beavo, J.A., and Rudensky, A.Y. (2007). Foxp3-dependent programme of regulatory T-cell differentiation. Nature *445*, 771–775.

Gondek, D.C., Lu, L.F., Quezada, S.A., Sakaguchi, S., and Noelle, R.J. (2005). Cutting edge: Contact-mediated suppression by CD4+CD25+ regulatory cells involves a granzyme B-dependent, perforin-independent mechanism. J. Immunol. *174*, 1783–1786.

Grimbaldeston, M.A., Nakae, S., Kalesnikoff, J., Tsai, M., and Galli, S.J. (2007). Mast cell-derived interleukin 10 limits skin pathology in contact dermatitis and chronic irradiation with ultraviolet B. Nat. Immunol. *8*, 1095–1104.

Guenther, M.G., Levine, S.S., Boyer, L.A., Jaenisch, R., and Young, R.A. (2007). A chromatin landmark and transcription initiation at most promoters in human cells. Cell *130*, 77–88.

Henderson, W.R., Jr., Banerjee, E.R., and Chi, E.Y. (2005). Differential effects of (S)- and (R)-enantiomers of albuterol in a mouse asthma model. J. Allergy Clin. Immunol. *116*, 332–340.

Henderson, W.R., Jr., Chi, E.Y., Bollinger, J.G., Tien, Y.T., Ye, X., Castelli, L., Rubtsov, Y.P., Singer, A.G., Chiang, G.K., Nevalainen, T., et al. (2007). Importance of group X-secreted phospholipase A2 in allergen-induced airway inflammation and remodeling in a mouse asthma model. J. Exp. Med. *204*, 865–877.

Henderson, W.R., Jr., Lewis, D.B., Albert, R.K., Zhang, Y., Lamm, W.J., Chiang, G.K., Jones, F., Eriksen, P., Tien, Y.T., Jonas, M., and Chi, E.Y. (1996). The importance of leukotrienes in airway inflammation in a mouse model of asthma. J. Exp. Med. *184*, 1483–1494.

Hori, S., Nomura, T., and Sakaguchi, S. (2003). Control of regulatory T cell development by the transcription factor Foxp3. Science (N. Y) *299*, 1057–1061.

Jankovic, D., Kullberg, M.C., Feng, C.G., Goldszmid, R.S., Collazo, C.M., Wilson, M., Wynn, T.A., Kamanaka, M., Flavell, R.A., and Sher, A. (2007). Conventional T-bet(+)Foxp3(-) Th1 cells are the major source of host-protective regulatory IL-10 during intracellular protozoan infection. J. Exp. Med. *204*, 273–283.

Kamanaka, M., Kim, S.T., Wan, Y.Y., Sutterwala, F.S., Lara-Tejero, M., Galan, J.E., Harhaj, E., and Flavell, R.A. (2006). Expression of interleukin-10 in intestinal lymphocytes detected by an interleukin-10 reporter knockin tiger mouse. Immunity *25*, 941–952.

Khattri, R., Cox, T., Yasayko, S.A., and Ramsdell, F. (2003). An essential role for Scurfin in CD4+CD25+ T regulatory cells. Nat. Immunol. *4*, 337–342.

Kim, J.M., Rasmussen, J.P., and Rudensky, A.Y. (2007). Regulatory T cells prevent catastrophic autoimmunity throughout the lifespan of mice. Nat. Immunol. *8*, 191–197.

Komatsu, N., and Hori, S. (2007). Full restoration of peripheral Foxp3+ regulatory T cell pool by radioresistant host cells in scurfy bone marrow chimeras. Proc. Natl. Acad. Sci. USA *104*, 8959–8964.

Kuhn, R., Lohler, J., Rennick, D., Rajewsky, K., and Muller, W. (1993). Interleukin-10-deficient mice develop chronic enterocolitis. Cell *75*, 263–274.

Kullberg, M.C., Hay, V., Cheever, A.W., Mamura, M., Sher, A., Letterio, J.J., Shevach, E.M., and Piccirillo, C.A. (2005). TGF-beta1 production by CD4+ CD25+ regulatory T cells is not essential for suppression of intestinal inflammation. Eur. J. Immunol. *35*, 2886–2895.

Li, M.O., Wan, Y.Y., and Flavell, R.A. (2007). T cell-produced transforming growth factor-beta1 controls T cell tolerance and regulates Th1- and Th17-cell differentiation. Immunity *26*, 579–591.

Lin, W., Haribhai, D., Relland, L.M., Truong, N., Carlson, M.R., Williams, C.B., and Chatila, T.A. (2007). Regulatory T cell development in the absence of functional Foxp3. Nat. Immunol. *8*, 359–368.

Mahic, M., Yaqub, S., Johansson, C.C., Tasken, K., and Aandahl, E.M. (2006). FOXP3+CD4+CD25+ adaptive regulatory T cells express cyclooxygenase-2 and suppress effector T cells by a prostaglandin E2-dependent mechanism. J. Immunol. *177*, 246–254.

Makela, M.J., Kanehiro, A., Borish, L., Dakhama, A., Loader, J., Joetham, A., Xing, Z., Jordana, M., Larsen, G.L., and Gelfand, E.W. (2000). IL-10 is necessary for the expression of airway hyperresponsiveness but not pulmonary inflammation after allergic sensitization. Proc. Natl. Acad. Sci. USA *97*, 6007–6012.

Marson, A., Kretschmer, K., Frampton, G.M., Jacobsen, E.S., Polansky, J.K., MacIsaac, K.D., Levine, S.S., Fraenkel, E., von Boehmer, H., and Young, R.A. (2007). Foxp3 occupancy and regulation of key target genes during T-cell stimulation. Nature *445*, 931–935.

Maynard, C.L., Harrington, L.E., Janowski, K.M., Oliver, J.R., Zindl, C.L., Rudensky, A.Y., and Weaver, C.T. (2007). Regulatory T cells expressing interleukin 10 develop from Foxp3(+) and Foxp3(−) precursor cells in the absence of interleukin 10. Nat. Immunol. *8*, 931–941.

Miyara, M., and Sakaguchi, S. (2007). Natural regulatory T cells: mechanisms of suppression. Trends Mol. Med. *13*, 108–116.

Moore, K.W., de Waal Malefyt, R., Coffman, R.L., and O'Garra, A. (2001). Interleukin-10 and the interleukin-10 receptor. Annu. Rev. Immunol. *19*, 683–765.

Nylen, S., Maurya, R., Eidsmo, L., Manandhar, K.D., Sundar, S., and Sacks, D. (2007). Splenic accumulation of IL-10 mRNA in T cells distinct from CD4+CD25+ (Foxp3) regulatory T cells in human visceral leishmaniasis. J. Exp. Med. *204*, 805–817.

Oderup, C., Cederbom, L., Makowska, A., Cilio, C.M., and Ivars, F. (2006). Cytotoxic T lymphocyte antigen-4-dependent down-modulation of costimulatory molecules on dendritic cells in CD4+ CD25+ regulatory T-cell-mediated suppression. Immunology *118*, 240–249.

Ohl, L., Mohaupt, M., Czeloth, N., Hintzen, G., Kiafard, Z., Zwirner, J., Blankenstein, T., Henning, G., and Forster, R. (2004). CCR7 governs skin dendritic cell migration under inflammatory and steady-state conditions. Immunity *21*, 279–288.

Paust, S., Lu, L., McCarty, N., and Cantor, H. (2004). Engagement of B7 on effector T cells by regulatory T cells prevents autoimmune disease. Proc. Natl. Acad. Sci. USA *101*, 10398–10403.

Powrie, F., Carlino, J., Leach, M.W., Mauze, S., and Coffman, R.L. (1996). A critical role for transforming growth factor-beta but not interleukin 4 in the suppression of T helper type 1-mediated colitis by CD45RB(low) CD4+ T cells. J. Exp. Med. *183*, 2669–2674.

Roers, A., Siewe, L., Strittmatter, E., Deckert, M., Schluter, D., Stenzel, W., Gruber, A.D., Krieg, T., Rajewsky, K., and Muller, W. (2004). T cell-specific inactivation of the interleukin 10 gene in mice results in enhanced T cell responses but normal innate responses to lipopolysaccharide or skin irritation. J. Exp. Med. *200*, 1289–1297.

Shevach, E.M., McHugh, R.S., Piccirillo, C.A., and Thornton, A.M. (2001). Control of T-cell activation by CD4+ CD25+ suppressor T cells. Immunol. Rev. *182*, 58–67.

Singh, B., Read, S., Asseman, C., Malmstrom, V., Mottet, C., Stephens, L.A., Stepankova, R., Tlaskalova, H., and Powrie, F. (2001). Control of intestinal inflammation by regulatory T cells. Immunol. Rev. *182*, 190–200.

Tang, Q., Boden, E.K., Henriksen, K.J., Bour-Jordan, H., Bi, M., and Bluestone, J.A. (2004). Distinct roles of CTLA-4 and TGF-beta in CD4+CD25+ regulatory T cell function. Eur. J. Immunol. *34*, 2996–3005.

Uhlig, H.H., Coombes, J., Mottet, C., Izcue, A., Thompson, C., Fanger, A., Tannapfel, A., Fontenot, J.D., Ramsdell, F., and Powrie, F. (2006). Characterization of Foxp3+CD4+CD25+ and IL-10-secreting CD4+CD25+ T cells during cure of colitis. J. Immunol. *177*, 5852–5860.

von Boehmer, H. (2005). Mechanisms of suppression by suppressor T cells. Nat. Immunol. *6*, 338–344.

Wan, Y.Y., and Flavell, R.A. (2007). Regulatory T-cell functions are subverted and converted owing to attenuated Foxp3 expression. Nature *445*, 766–770.

Wildin, R.S., and Freitas, A. (2005). IPEX and FOXP3: Clinical and research perspectives. J. Autoimmun. Suppl. *25*, 56–62.

Williams, L.M., and Rudensky, A.Y. (2007). Maintenance of the Foxp3-dependent developmental program in mature regulatory T cells requires continued expression of Foxp3. Nat. Immunol. *8*, 277–284.

Zhang, Y., Lamm, W.J., Albert, R.K., Chi, E.Y., Henderson, W.R., Jr., and Lewis, D.B. (1997). Influence of the route of allergen administration and genetic background on the murine allergic pulmonary response. Am. J. Respir. Crit. Care Med. *155*, 661–669.

Zheng, Y., Josefowicz, S.Z., Kas, A., Chu, T.T., Gavin, M.A., and Rudensky, A.Y. (2007). Genome-wide analysis of Foxp3 target genes in developing and mature regulatory T cells. Nature *445*, 936–940.